Bioresource Technology Reports 20 (2022) 101264

Contents lists available at ScienceDirect

Bioresource Technology Reports

journal homepage: www.sciencedirect.com/journal/bioresource-technology-reports

Potential role of sulfide precipitates in direct interspecies electron transfer facilitation during anaerobic digestion of fish silage

Behnam Hashemi [a,*], Svein Jarle Horn [b,c], Jacob J. Lamb [a], Kristian M. Lien [a]

[a] Department of Energy and Process Engineering & ENERSENSE, NTNU, Trondheim, Norway
[b] Faculty of Chemistry, Biotechnology, and Food Science, Norwegian University of Life Sciences (NMBU), 1432 Ås, Norway
[c] NIBIO, Norwegian Institute of Bioeconomy Research, Frederik A. Dahls vei 20, 1432 Ås, Norway

ARTICLE INFO

Keywords:
Anaerobic digestion
Iron sulfide
XRD analysis of digestate
Bacteria syntrophic consortia
Mackinawite
Greigite

ABSTRACT

Fish waste (FW) contains large amounts of protein and is a challenging feedstock for biogas production due to possible H_2S and ammonia generation. Adding $FeCl_3$ to an anaerobic digester can precipitate H_2S. Mackinawite and greigite are conductive and magnetic substances formed from H_2S precipitation. Direct interspecies electron transfer (DIET) can be stimulated by developing these conductive materials and by applying an external magnetic force. In this study, FW was digested in batch reactors and exposed to magnets magnetic fields from 3 to 115 mT. The results showed that the use of magnetic fields could increase the biomethane yield by up to 36 %. XRD analyses showed that mackinawite and greigite were accumulating in the solid phase in digesters added $FeCl_3$. Genetic analysis of the microbial community suggested that applying a magnetic field not only increased the relative abundance of protein-hydrolyzing bacteria but also potentially improved methane production through DIET.

1. Introduction

The fishery industry plays an essential role in many economies, including China, India, Spain, the USA, Canada, and Norway (Ahuja et al., 2020). According to The Food and Agriculture Organization of the United Nations (FAO) report in 2020, global fish production (aquaculture and wild fish) increased from 166 million tonnes in 2016 to 178.5 million tonnes in 2018. From that, around 2.5 million tonnes were produced in Norway (Organization of the United Nations (FAO), 2020). Raw fish is processed by employing various techniques to enable human consumption. Using these techniques leads to the generation of a vast amount of residues, including head, skin, intestines, bones, eggs, blood, and skin that account for approximately 27 % of fish weight (Sarker, 2020; Stevens et al., 2018). In addition, the by-products of fish production, including fish sludge (i.e., mainly from remaining fish feed, dead or slaughtered fish), are a large portion of aquaculture fish waste (Aas, 2016). Even though a significant portion of this waste has high nutritional value, it is disposed of as landfill or incinerated, polluting water or emitting toxic gases (Sarker, 2020). To mitigate the environmental effects created by fish waste landfills or incineration, several alternatives for fish waste management have been proposed in which fish waste is consumed as the primary source for energy production.

Fish waste is rich in organic materials, including proteins and fats, making it suitable to be converted to biogas (i.e., mainly CH_4 and CO_2) through a biological process called anaerobic digestion (AD) (Solli et al., 2018). AD refers to a complex biochemical process that is carried out by a consortium of microorganisms (B. Hashemi et al., 2021). AD includes four main steps, 1) hydrolysis, 2) acidogenesis, 3) acetogenesis, and 4) methanogenesis (Metcalf et al., 2014). The first three steps refer to biological and chemical reactions where particles are dissolved, and biopolymers are converted to volatile fatty acids (VFAs), simple alcohols (e.g., ethanol and methanol), and acetate (B. Hashemi et al., 2021). Methanogenesis is a biological process for production of methane from different intermediates in the AD process; 1) acetoclastic (where acetate is converted to methane and carbon dioxide), 2) hydrogenotrophic (where molecular hydrogen and carbon dioxide are converted to methane and water), 3) methylotrophic (where methanethiol or methylamine are converted to methane and CO_2, and 4) recently discovered direct interspecies electron transfer (DIET) where electrons are obtained from a direct partnership with bacteria and used to convert CO_2 to methane (Dubé and Guiot, 2015; Feng et al., 2022; S. Hashemi et al., 2021). The reaction mechanisms of the different types of methanogenesis pathways are summarized in Table 1.

Among all the microbes involved in AD, methanogenic archaea play

* Corresponding author.
E-mail address: seyedbehnam.hashemi@ntnu.no (B. Hashemi).

https://doi.org/10.1016/j.biteb.2022.101264
Received 19 September 2022; Received in revised form 22 October 2022; Accepted 27 October 2022
Available online 2 November 2022

Table 1
Mechanisms of different methanogenesis pathways.

Pathway	Reaction equation
Hydrogenotrophic methanogenesis	$4H_2 + CO_2 \rightarrow CH_4 + 2H_2O$
Acetoclastic methanogenesis	$CH_3COO^- + H^+ \rightarrow CH_4 + CO_2$
Methylotrophic pathway (amine)	$4CH_3NH_2 + 2H_2O \rightarrow 3CH_4 + CO_2 + 4NH_3$
DIET pathway	$9H^+ + 8e^- + CO_2 \rightarrow CH_4 + 2H_2O$

an essential role since they are the only group of microbes that can form methane (Cai et al., 2021). In the acetoclastic pathway, methane and carbon dioxide are generated, and the reaction yields −31 kJ/mol for cell maintenance and reproduction. In the hydrogenotrophic pathway, H_2 acts as an electron donor and combines with CO_2 to generate methane that yields −135.6 kJ/mol (Kadota et al., 2019). According to the mechanisms of these two pathways, in acetoclastic methanogenesis, 1 mol of CO_2 is released per 1 mol of acetate consumed. In contrast, in hydrogenotrophic methanogenesis, 1 mol of CO_2 is consumed with 4 mol of molecular H_2 to produce methane and water (Sikora et al., 2017). Therefore, while acetoclastic methanogenesis produces CO_2, hydrogenotrophic methanogenesis can reduce net CO_2 in the system.

Methanogenesis from acetate follows two pathways, acetate, and syntrophic acetate oxidation (SAO) (Frank et al., 2016). In the acetate pathway, acetate will be converted to methane and CO_2 (Table 1). The two-step SAO pathway includes acetate oxidation ($CH_3COOH + 4H_2O \rightarrow 2CO_2 + 4H_2$, $\Delta G^0 = +104.6$ kJ/mol) to H_2 and CO_2 followed by hydrogenotrophic methanogenesis (Dyksma et al., 2020).

The SAO pathway is thermodynamically unfavorable under standard conditions; however, this reaction can be favorable if hydrogenotrophic methanogenesis reduces the hydrogen pressure through interspecies hydrogen transfer (IHT) (Sikora et al., 2017). Hydrogen and formate transfer are two possible mechanisms for IHT (Kumar et al., 2021). Formate transfer is more likely when SAO bacteria and hydrogenotrophs are not in close contact. Hydrogen transfer is more favorable when the distances are shorter (Lv et al., 2020; Wang and Lee, 2021). Thus, the overall reaction for SAO becomes exergonic, with similar stoichiometry to the acetate reaction (Dubé and Guiot, 2015). The acetoclastic pathway is mainly carried out with *Methanothrix* and *Methanosarcina* spp. (Jin et al., 2019). In comparison, SAO is performed by the close relationship between bacteria belonging to Firmicutes phylum (e.g., *Clostridium*, *Syntrophaceticus*, *Tepidanaerobacter*, *Thermacetogenium*, *Thermotoga*, and strain AOR) and hydrogenotrophic methanogens (e.g., *Methanomicrobiales* spp., *Methanobacteriales* spp., *Methanococcales* spp., *Methanosarcinaceae* spp., *Methanoculleus* and under certain conditions also *Methanosarcina*) (Fotidis et al., 2013). Elevated ammonia level (from 1.7 to 14 g/L) inhibits the function of acetoclastic methanogens by a change in intracellular pH, increase in energy requirement, and depletion of intracellular potassium (Fotidis et al., 2013).

In DIET, the c-type cytochromes and pili in the outer membranes are involved in cell-to-cell electron transfer. *Methanosarcina* and *Methanothrix* (formerly *Methanosaeta*), well-known DIET partners, do not possess outer surface c-type cytochromes or e-pili; therefore, their outer-surface contact for DIET is not clear (Wagner et al., 2017; Yan and Ferry, 2018). It is proposed that a specific concentration of *Methanophenazine* (i.e., a redox-active metallic ion capable of electron transfer in some methanogens) in the membrane of some species belonging to *Methanosarcina* can convert them to electrically conductive materials that may reduce the requirements for active redox proteins (Holmes et al., 2018; Wagner et al., 2017). For the first step of CO_2 reduction to methane, *Methanosarcina* needs to produce reduced ferredoxin (Holmes et al., 2018). It is suggested that the oxidation of reduced ferredoxin is essential not only for electron transfer via the membrane in *Methanosarcina* but also to increase the concentration of crucial enzymes (e.g., acetyl-CoA) for degradation of the non-gaseous products of acidogenesis (Buckel and Thauer, 2018; Sikora et al., 2017).

Under typical AD conditions (using simple organic materials as substrate), the hydrogenotrophic methanogenesis are responsible for about one-third of total methane production (S. Hashemi et al., 2021). In contrast, harsh operating conditions such as using high ammonia containing fish waste as substrate yields a process where methanation is typically dominated by the hydrogenotrophic route rather than the acetoclastic one (Wang et al., 2020). This has conventionally been interpreted to mean that the hydrogen concentration in the reactor will be crucial for reactor productivity. If it is too high, then the reactor will turn sour due to fatty acids accumulation, inhibiting further methanogenic activity. If it is too low, then the methanogens will starve and stop multiplying, and then end up being washed out of the reactor (Stams and Plugge, 2009; Z. Wang et al., 2021).

Lately, it has been recognized that the hydrogenotrophic route does not necessarily involve explicit hydrogen transfer among bacteria and archaea. In the so-called DIET transfer process, electrons are exchanged instead of hydrogen molecules (Z. Wang et al., 2021). This is kinetically a much faster process (electrons move rapidly compared to the larger hydrogen molecules), and it is also thermodynamically more efficient (inevitable energy losses associated with the production and consumption of intermediate hydrogen molecules are avoided) (Sikora et al., 2017). In some AD processes, DIET can naturally occur through biologically produced pili and outer membrane cytochromes (Lamb et al., 2014; Lamb and Hohmann-Marriott, 2017). It is, however, of interest to investigate the potential of DIET through engineered methods such as transfer via a conducting surface from an electron donor bacterium to an electron recipient archaea. Many recent studies have reported stimulation of the DIET process by adding conductive material surfaces such as active carbon, carbon cloth, carbon nanotubes, charcoal, magnetite, and other conductive materials (Baek et al., 2019; Barua and Dhar, 2017; Dubé and Guiot, 2015; Kumar et al., 2021; Li et al., 2019).

It is often overlooked that sulfur containing substrates, such as proteins, may generate their own conductive surfaces (Gramp et al., 2010). When the sulfur contents of proteins are digested, hydrogen sulfide (H_2S) is released, which is highly toxic to humans, and detrimental to the activity of many microorganisms. Sulfur-reducing-bacteria compete with hydrogenotrophic archaea on hydrogen. Iron chloride is often added to precipitate the hydrogen sulfide as solid iron sulfides. These sulfides may be formed in many different ways, but a typical reaction scheme may be the following (Picard et al., 2018; Su et al., 2015):

$$H_2S + FeCl_3 \rightarrow \text{mackinawite } (FeS) \rightarrow \text{greigite } (Fe_3S_4) \rightarrow \text{pyrite } (FeS_2).$$

Pyrite is thermodynamically the most stable form of iron sulfide, but pyrite formation during AD is very limited (Su et al., 2015). The main sulfide formation during AD will be a mixture of mackinawite and greigite, which are both electron conducting solids (Skyllberg et al., 2021). Furthermore, greigite (Fe_3S_4) is the sulfur analogue of magnetite (Fe_3O_4), which both are materials exhibiting pronounced ferrimagnetism (Roldan et al., 2013). Recognizing that electron transfer (i.e., motion of charged particles) and emergence of magnetic fields are two sides of the same coin, it should therefore be anticipated that the presence of ferrimagnetic materials could impact the DIET process (L. Li et al., 2022; Martins et al., 2018). Stimulation of this process could be considered in different ways, including application of external magnetic fields, as well as magnetic separation and recycling of magnetic material together with the associated electron-transferring microorganisms. The efficiency of the circulation of conductive elements such as greigite and mackinawite with external magnetic force depends on the size and concentration of these materials. The magnetic field may aid development and accumulation of the magnetic elements in AD.

Iron sulfides have hydrophilic surfaces and are porous, making them suitable for growing biofilms (i.e., a thin layer of a self-produced matrix of syntrophic microorganisms that adhere to each other and a surface). The surface of materials exhibiting pronounced ferrimagnetism provides large positive charges that attract negatively charged microorganisms (Hellman et al., 2010). In addition, an external magnetic force may concentrate the elements formed in the reaction mentioned above and

provide larger nanocrystals with an expanded surface for biofilm aggregation and growth, potentially resulting in an improved DIET process.

Electrotrophic methanogens can accept electrons directly from other species (Lovley, 2022). On the other hand, *Geobacter* species actively participate in DIET. These bacteria can form a biological bridge to transfer electrons to methanogens by making microbial nanowires (also known as electrically conductive pili or e-pili) (Holmes et al., 2018). The addition of conductive non-biological materials as electroactive media (e.g., char, activated carbon, iron nanoparticles, and magnetic crystals) can stimulate DIET in a wide range of syntrophic bacteria that cannot build microbial nanowires like *Geobacter* species. Syntrophic partners within Firmicutes and Proteobacteria can attach to the surface of the electroactive media and employ them as electrical conduits for electron transfer (Park et al., 2018). This approach is metabolically more favorable since microbes invest less energy than they would for generating conductive pili. In this way, methanogens have more energy to dedicate to cell growth, resulting in greater methanogens abundance and higher methane production potential (Park et al., 2018). The syntrophic bacterial partners may include *Proteobacteria*, *Firmicutes*, and *Coprothermobacteraeota* phyla members. This includes microorganisms belonging to *Geobacter*, *Shewrnelia*, *Desulfovibrio*, and *Clostridium*. On the other hand, methanogenic archaea known to be part of DIET belong to the families *Methanobacteriaceae*, *Methanomassiliicoccaceae*, *Methanothrix*, *Methanosarcinaceae*, and *Methanothermobacteraceae*. Different studies have previously assessed the effect of adding magnetic elements (magnetite) and applying an external magnetic field on microbial community dynamic and biomethane yield (Chen et al., 2019; Kato et al., 2012; Masood, 2017; D. Wang et al., 2018). The effect of applying an external magnetic field on the microbial community in a system with mackinawite and greigite as the electroactive media for DIET in AD is not fully understood. In this study, protein-rich fish waste (FW) was utilized as the AD system's primary substrate and the main sulfide source. The hypothesis was that the magnetic and/or conductive substances (i.e., greigite and mackinawite) could be developed in the digesters when adding $FeCl_3$. Moreover, possible improvements in biomethane yield due to potential establishment of DIET were investigated. Additionally, this study investigated if applied magnetic fields could create/concentrate larger conductive and magnetic crystals of mackinawite and greigite that microorganisms can use as the electroactive media promotes the DIET metabolism.

2. Material & methods

2.1. Substrate

Protein- and fat-rich fish waste (FW) was employed as the main feedstock in this study. The substrate was collected from a biogas production plant at the west of Norway. As a result of the pre-treatment, the substrate had a pH of 4.2, and was a homogeneous liquid. Before adding fish waste to the reactors as feedstock, FW was diluted with distilled water to reduce the volatile solids (VS) content to 15 ± 1 %.

2.2. Inoculum

The inoculum needed for AD start-up was collected from a commercial biogas plant in the west of Norway. The operational temperature of the reactor was 40 °C, and FW served as the main substrate for the reactor. The inoculum was stored at 40 °C for 20 days to minimize endogenous biogas production. The pH of the inoculum before AD was 8.1. The physical and chemical properties of the start-up inoculum are summarized in Table 2, which also includes the properties of the feedstock.

2.3. Reactor design for anaerobic digestion

2.3.1. Biomethane potential test

Batch AD was conducted based on a modified protocol, ISO 11734 (1995), according to Møller et al., to investigate possible improvement of biogas production as a consequence of applying a magnetic field (Møller et al., 2004). All the parameters, including substrate and inoculum load, temperature, and mixing condition, were similar in all digesters. Briefly, a half-liter glass bottle was used as an anaerobic digester. Permanent magnets were installed on the outer surface of the bottles to provide the magnetic field as described in the following subsection. 200 g of inoculum was added to the bottles, and the substrate was added to reach a substrate to inoculum ratio (S:I) of 0.5. The headspace of the reactors was flushed with pure nitrogen to ensure an anaerobic environment, and then the bottles were sealed by air-tight caps. Reactors were fed twice over 65 days. After 30 days of adaptation of the reactors, in the second feeding step, 0.01 mM $FeCl_3$ was added to the substrate to facilitate H_2S precipitation. The reactors were continuously mixed at 100 rpm in an Infors Minitron shaking incubator (Infors, Bottmingen, Switzerland) and kept at 40 °C. Each experiment was conducted in triplicate.

2.3.2. Magnetic field

Magnetic fields were applied using permanent magnet discs provided by SuperMagneter AS (Kristiansand, Norway). Three different neodymium magnets (N38) were used, as indicated in the Fig. 1. Magnets were named weak (FW_WM, Ø4 × 4 mm), moderate (FW_MM, Ø7 × 3 mm), and strong (FW_LM, Ø10 × 4 mm), corresponding to their maximum magnetic force (i.e., 5.5, 10 and 21 N, respectively). The magnetic fields in the reactors were estimated using an online magnet field calculator provided by Integrated Magnetics (CA, USA). To simplify flux density calculations, it is assumed that two magnet fields face each other in an attractive position. The reactors were divided into four zones, each with a 1 cm thickness, as illustrated in Fig. 1. The maximum and minimum magnetic flux densities (milli-Tesla, mT) were calculated in each zone for different magnets and stated in Fig. 1. Three reactors were used as controls without magnets to draw a baseline for the biogas production. The design parameters utilized for the experimental setup are given in Table 3.

2.4. X-ray diffraction

After finishing the BMP tests, the content of each bottle was centrifuged, and a solid digestate was collected for crystal analysis. The aim was to investigate the greigite and mackinawite content of the solid digestate.

2.4.1. Sample preparation

To avoid any change in the structure of components, the solid digestate was snap-frozen using liquid nitrogen. The content was then freeze-dried using a Labconco FreeZone 2.5-liter freeze-dryer (MO, USA). The freeze-dried samples were pulverized using a millstone and

Table 2
Physical and chemical characteristics of fish waste.

	Total solid (TS) %	Volatile solids (VS) %	Carbohydrates % TS	Proteins % TS	Fats % TS	NH_4-N g/kg	S g/kg	pH
Fish waste	64.4	61.9	13.1	11.3	59.9	1.2	4.2	4.2
Inoculum	4.43	3.7	5.3	1.61	24.2	0.6	3.7	8.1

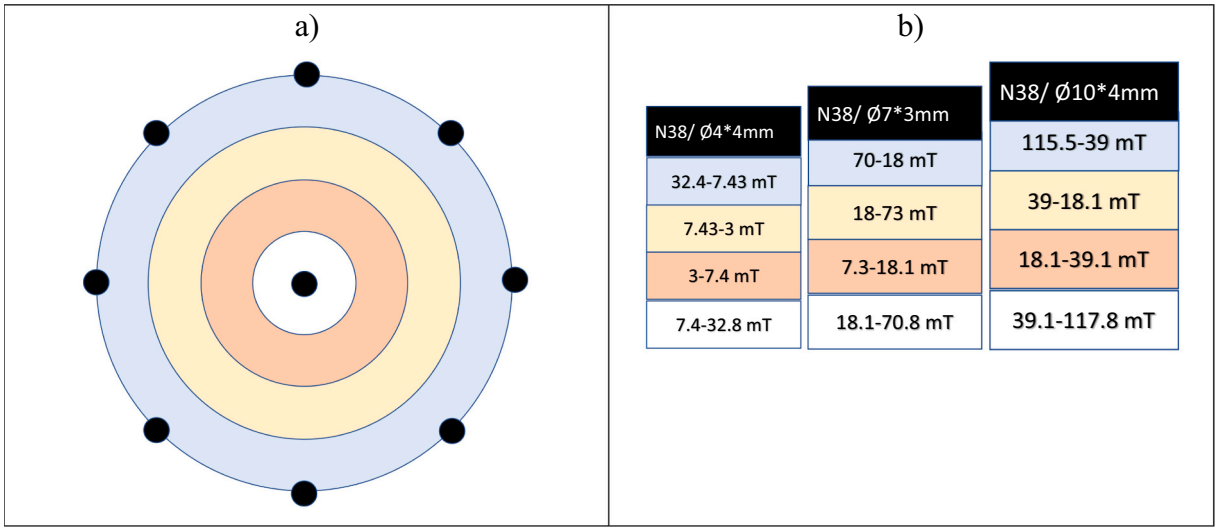

Fig. 1. Position of each magnet and zones of different magnetic fluxes (a), and the calculated magnetic flux inside each reactor based on magnet strength (b). WM: N38/Ø4 * 4 mm; MM: N38/Ø7 * 3 mm; SM: N38/Ø10 * 4 mm. Magnets were located on the batch reactors' surface to provide a homogenized magnet field in the entire working volume. Seventeen magnet discs (WM, MM, and SM) were installed for each reactor. Apart from the central magnet installed precisely on the center of the bottom surface (outside of the reactor), the rest were arranged in two rows, one at the height of 2 cm and the other at 4 cm from the bottom. The magnets' distance is considered to have the least neutralizing effect. To simplify the calculations, the glass thickness gap between magnet and liquid (2 mm) was considered air instead of glass.

Table 3
Experimental set-up. Four different experiments were prepared in triplicate with fish waste (FW) as substrate; one experiment without applying a magnetic field (FW), one using a weak magnet field (FW_WM), one with a moderate magnet (FW_MM), and one with a strong magnet (FW_SM), In the first run, $FeCl_3$ was not employed in the reactors. In contrast, the second run $FeCl_3$ solution was added to the reactors. The substrate to inoculum ratio (S:I) in all the samples was approximately 0.5. Flux density was calculated via online calculators as described before. Three samples with only inoculum prepared, and the biogas produced from these samples was subtracted from all other experiments.

Sample ID	Experiments	Flux density mT	First run			Second run			
			Inoculum gr VS	Substrate gr VS	S:I	Inoculum gr VS	Substrate gr VS	S:I	$FeCl_3$ mM
Ino.	Only inoculum	0	8	–	–	8	–	–	–
FW	No magnet	0	8 ± 0.3	4 ± 0.05	0.5	8 ± 0.1	4	0.5	0.1
FW_WM	Weak magnet	7.4–43	8 ± 0.2	4 ± 0.05	0.5	8 ± 0.1	4	0.5	0.1
FW_MM	Moderate magnet	7.3–70.8	8 ± 0.2	4 ± 0.02	0.5	8 ± 0.2	4	0.5	0.1
FW_SM	Strong magnet	18.4–118	8 ± 0.1	4 ± 0.03	0.5	8 ± 0.1	4	0.5	0.1

stored in vacuum bottles with self-sealing silicone caps at room temperature before further analysis.

2.4.2. X-ray diffraction analysis

Powder X-ray diffraction (XRD) was performed using a Bruker D8 A25 DaVinci X-ray Diffractometer with CuKα radiation and LynxEye™ SuperSpeed Detector equipped with a 90-position sample changer. Samples were packed into a zero-background sample holder and step-scanned from 10 to 90° 2θ using a step size of 0.02° 2θ for 120 min. Two different databases were used to search and match for mackinawite and greigite. First, a COD database or Crystallography Open Database (http://www.crystallography.net/cod/) was employed to search for elements resulting in the identification of mackinawite at 13.02° 2θ. Finally, the other Theta points dedicated to greigite and mackinawite were identified using a PDF (Powder Diffraction File) by a licensed ICDD-4 database (https://www.icdd.com/pdf-4/).

2.5. Genetic analysis of microbial culture

Genetic analysis of the initial and final time points of each experiment were conducted to track changes in the microbial community.

2.5.1. DNA extraction and quantification

10 mL of the liquid samples were taken from each digester on the first day and day 65 to assess microbial culture changes due to applying a magnetic field. The liquid samples were snap-frozen using liquid nitrogen and stored at −80UNIT before the genetic analysis. Microbial community analysis was carried out by DNASense ApS (Aalborg Øst, Denmark). DNA extraction was conducted using the standard protocol for FastDNA spin kit for soil (MP Biomedicals, USA), described by Albertsen et al. (2015). The ultimate DNA purification was determined by Gel electrophoresis using Tapestation 2200 and D1000/High sensitivity D1000 screencaps (Agilent, USA). The DNA concentration was also measured by a Qubit dsDNA HS/BR Assay kit (Thermo Fisher Scientific, USA).

2.5.2. 16s RNA gene amplicon sequencing

Region 4 abV4-C amplificon library was prepared for the bacteria/archaea 16S RNA gene, based on the illumine protocol (illumine 2015). Ten ng extracted DNA was used as a template. The PCR (polymerase chain reaction) amplification was conducted with tailed primers according to Illumina, and contained primers targeting the bacteria/archaeal 16S rRNA gene variable region 4 (abV4-C): [515FB] GTGYCAGCMGCCGCGGTAA and [806RB] GGACTACNVGGGTWTCTAAT (Apprill et al., 2015). After extracting the sequencing libraries from PCR,

the results were quantified and purified. The purified amplicons were pooled in equimolar concentration and diluted to 2 nM, and then paired-end sequenced (2 × 300 bp) on a illumine MiSeq platform (Illumina, San Diego, USA) following the standard guidelines for preparation and loading samples on MiSeq.

2.6. Analysis

Daily biogas production was measured using a GMH 3161 pressure meter (Greisinger electronic, Regenstauf, Germany). 20 mL of biogas was collected in a gastight syringe and injected in a GA2000 Landfill Gas Analyzer (Geotechnical Instruments Ltd., UK) for biogas composition analysis (vol% of CO_2 and CH_4). The pH of the reactor was measured at the end of each week by taking a 2 mL sample and using pH test strips (Micro Essential Laboratory, NY, USA). The substrate and inoculum's total solids and volatile solids content were determined according to the standard protocols International and European Organizations for Standardization (ISO 10390: 2005; ISO 11465: 1993). For ammonium (NH_4) concentration analysis, 2 mL of liquid sample was taken from the bottles after 30 days. The samples were centrifuged at 15000 rpm for 10 min. The liquid supernatant was separated and diluted ten times before analysis. The NH4 concentration was measured using a photometric 5.2–103 mg/L cell test (Merck group, Germany) and a Spectroquant® Prove 100 spectrophotometer. Volatile fatty acids (VFA) were analyzed using high-performance liquid chromatography (HPLC) (Phenomenex, Torrance, Ca, USA) equipped with a 3000RC column. The HPLC operated at 85 °C and UV detection at 210 nm (Dionex, Sunnyvale, CA, USA). The samples' hydrogen sulfide (H_2S) was determined by collecting gas samples in a Kitagawa AP-20 portable sampling pump equipped with Kitagawa gas detector tube 120-SB (Kanagawa, Japan). Other properties including carbohydrates, proteins and fats were evaluated by Eurofins AS (Trondheim, Norway).

3. Results and discussion

3.1. Anaerobic digestion

Results regarding biogas production rate and H_2S reduction because of the $FeCl_3$ addition are provided in this section.

3.1.1. Biomethane production rate

AD of the FW was conducted in two main steps. In the first step, the aim was to adapt the microbial community to the magnetic fields. It is worth noting that the original inoculum might include some magnetic crystals (e.g., greigite and magnetic pyrite) due to the use of $FeCl_3$ in the biogas plant for H_2S management. In the second run, the aim was to assess the response of the microbial community to addition of $FeCl_3$ and to investigate possible improvements of biogas production rate.

Except for the reactors with strong magnets (SM), the methane produced in each rector in the first run was like the control reactors (Fig. 2a). At the end of the first period, a jump in methane production occurred in the SM reactors. The biomethane production increased from 458.8 mL/g VS in control samples to around 534 mL/gVS, resulting in a 16.4 % increase in methane production. After adding $FeCl_3$ to the

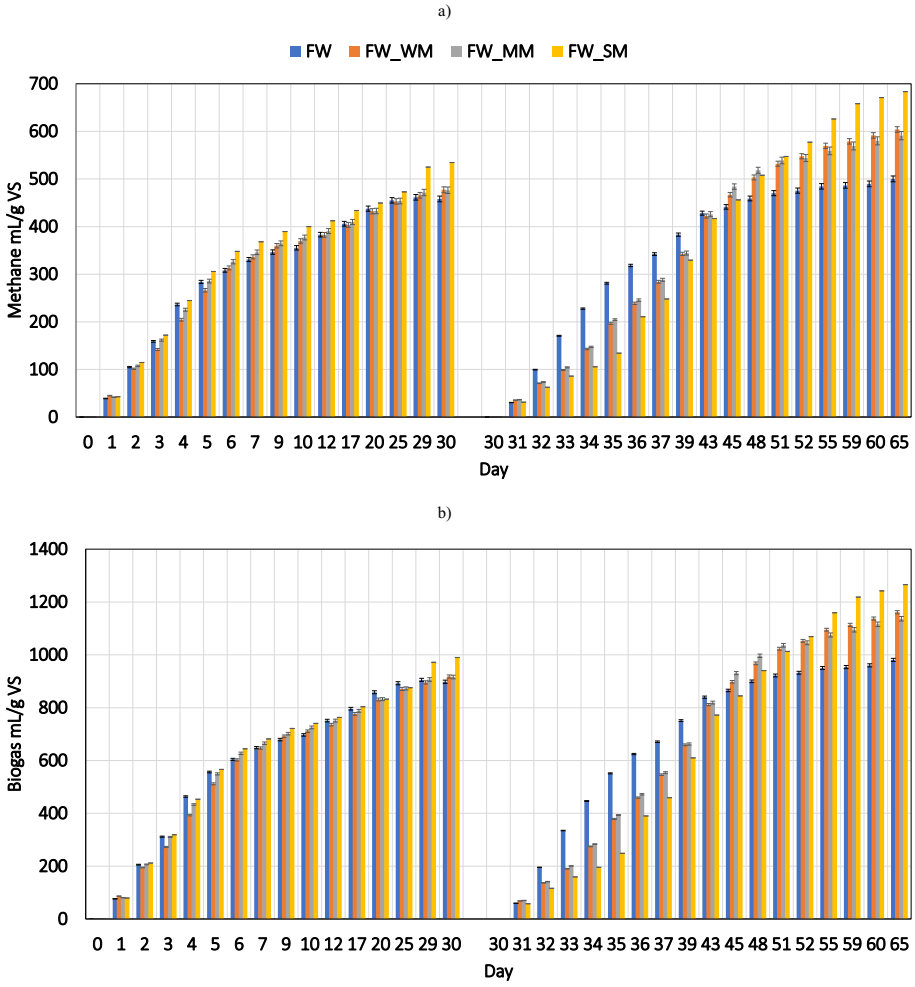

Fig. 2. The accumulative methane production yield in two feeding steps (a), and biogas production rate within two AD periods (b).

reactors in the second feeding, the final accumulative methane production was higher for all the experiments using magnets. The experiments with SM increased the methane yield from 501 mL/g VS to 683 mL/gVS (36 % increase). Experiments with the weak magnet (WM) and moderate magnet (MM) also showed improvements in methane production, increasing by 20.5 and 18 % (604 and 591 mL/g VS), respectively. The theoretical methane production of the FW was calculated using values of 415, 496, and 1014 mL/g for carbohydrates, proteins, and lipids, respectively (Møller et al., 2004). Based on data in Table 2, the maximum theoretical methane production from FW was estimated to 718 mL/g using data provided by (Møller et al., 2004). The maximum methane produced in experiments with SM reached 95 % of FW's theoretical methane production yield. The value for the control reactor was around 70 %.

Biogas production rate is an essential factor to consider in designing AD processes. Fig. 2b shows the samples' biogas production rate during the two feeding steps. All the samples had a similar production rate in the first feeding phase. The biogas production rate in the samples with magnets was reduced in the second feeding phase, where $FeCl_3$ solution was added together with the FW to the system. The accumulated biogas production on day 35 for the samples without magnets was 551 mL/g VS, while the value for samples with weak, moderate, and strong magnets was 378.8, 393, and 248 mL/g VS, respectively. This initial lower biogas production may be linked to the initial adaptation of microorganisms due to exposure to magnetic fields and $FeCl_3$. In contrast, in the second half of the experiment, the maximum daily biogas production in samples with magnets reached 152, 156, and 161 mL/g VS/Day for WM, MM, and SM, respectively. These values are much higher than the maximum biogas production yield of samples without magnets (88.3 mL/g VS/Day).

3.2. Hydrogen sulfide concentration

The H_2S content of different biogas samples are provided in Fig. 3. In the first digestion trials without $FeCl_3$ added, the hydrogen sulfide was above 65 ppm in the first week, dropping to around 50 ppm and staying almost unchanged in all the samples except for FW_SM, which dropped to 40 ppm. The H_2S concentration in digesters containing magnets was higher than in digesters without magnets on day 33. This may explain the lower biogas production rate of the magnet digesters at the beginning of the second batch test. On day 33, the maximum H_2S concentration for WM, MM, and SM was 69, 71, and 72 ppm, and these values were reduced to below 10 ppm in all the samples at the end of the experiment. H_2S concentration of samples without a magnet in the second round of experiments was 60 ppm and dropped to 27 ppm at the end of the investigation. The positive effect of $FeCl_3$ on reducing H_2S concentration in produced biogas is well documented in previous research, and our results are in line with the literature data (Choong et al., 2016; Erdirencelebi and Kucukhemek, 2018; Luo et al., 2022) However, the H_2S reduction in experiments with magnet was clearly higher than experiments without magnet.

3.3. XRD analysis of solid content

It is assumed that the magnetic field in AD reactors can improve the concentration and/or development of conductive and magnetic surfaces such as mackinawite and greigite in an anoxic environment. The magnetic field may also create currents in the crystals and thus improve DIET. These hypotheses were assessed during AD of FW by Magnetic discs. After AD, the solid content of each reactor was collected by centrifugation and snap-frozen using liquid nitrogen. After freeze-drying the samples, the solid materials were milled to make samples more homogenous to reduce the background noises in XRD results. Fig. 4 shows the XRD analysis of samples from the AD of FW and $FeCl_3$ with/without a magnetic field applied. Presence of mackinawite and greigite were targeted using a Diffraction EVA (V6.0.0.6) search and match software. The results were in line with literature data (Chang et al., 2008, 2011; Gallegos et al., 2007; Jeong et al., 2008; Mullet et al., 2002; Roberts et al., 2006; van Dongen et al., 2007). Different samples had different content of mackinawite and greigite. In the experiments without magnetic fields, mackinawite is the most abundant component in the system. In comparison, in some specific 2Theta ranges for MM and SM, the concentration of mackinawite decreased. At the same time, the number of greigite atoms increased. Therefore, greigite is the major constituent of the samples with MM and SM, but mackinawite is also abundant. This conversion of mackinawite to greigite was more pronounced as the magnetic field strength increased. In AD, greigite can be produced through a complex reaction from mackinawite, which is a time-dependent reaction. Picard et al. showed that in pure anoxic culture and the in presence of appropriate microorganisms (sulfate-reducing bacteria, SRB), it takes five months to observe greigite in the system (Picard et al., 2018). Mackinawite structure consists of micrometre-sized irregular aggregates composed of many flake-like nanoparticles (Ning et al., 2013; Ohfuji and Rickard, 2006). In contrast, greigite has a more well-defined crystal structure which is thermodynamically metastable (Vasiliev et al., 2008; Wang and Chen,

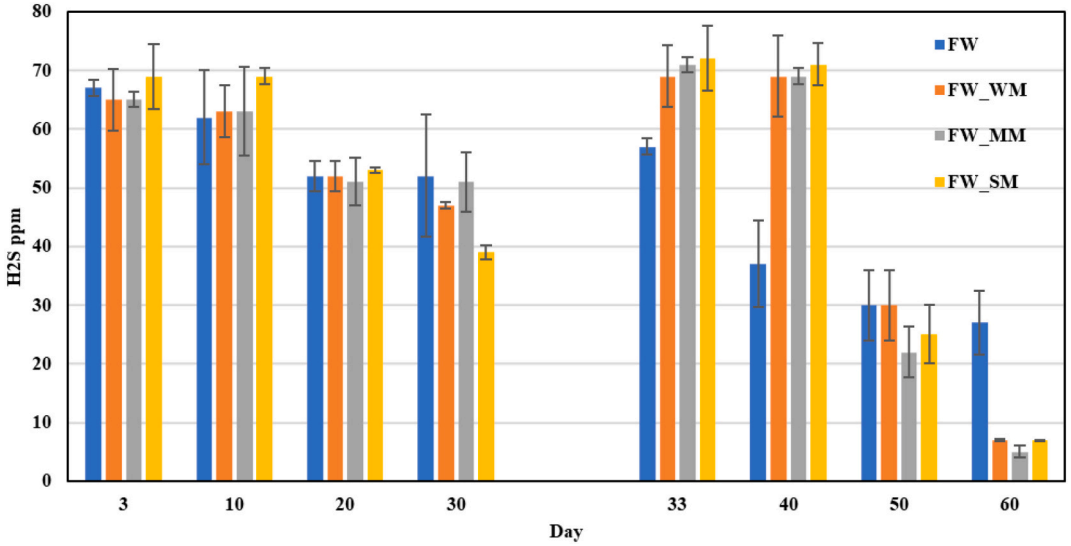

Fig. 3. Concentration of hydrogen sulfide in the produced biogas collected at different time points.

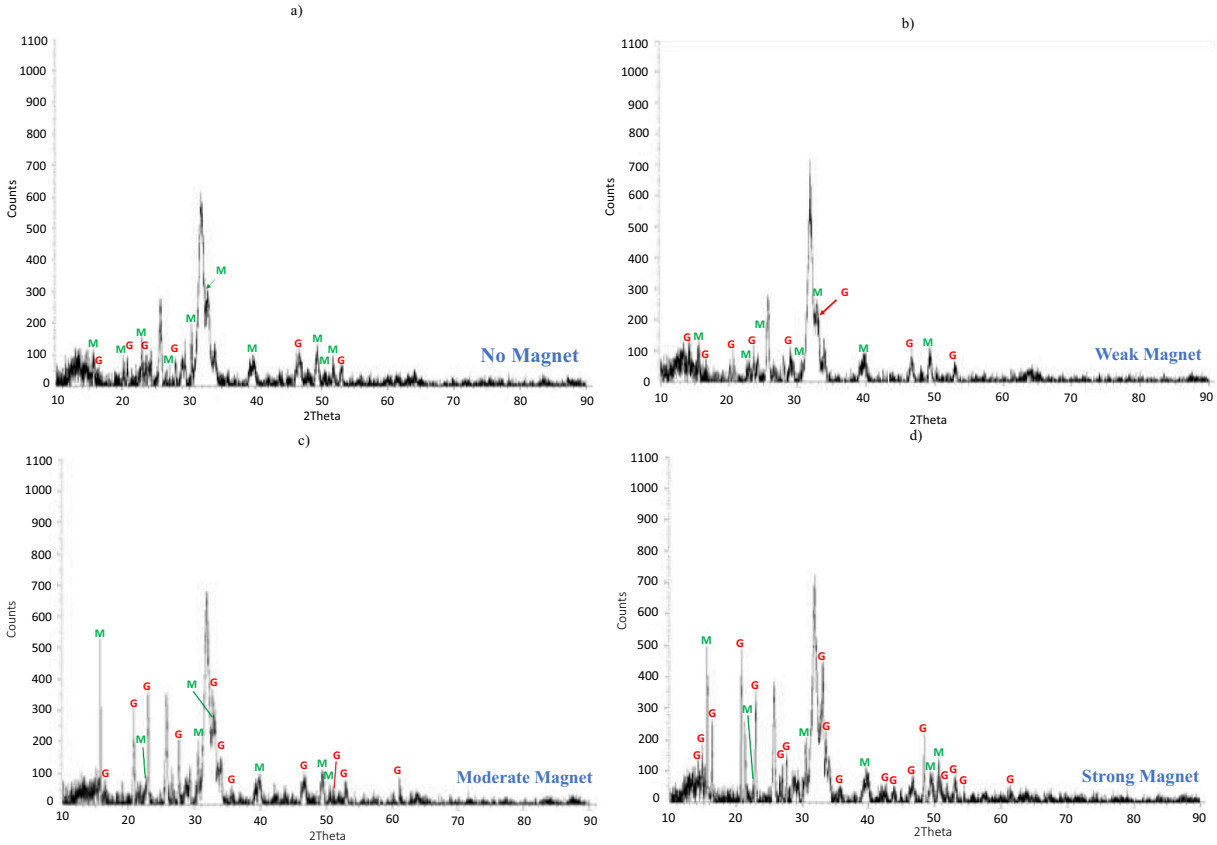

Fig. 4. XRD patterns for solid samples of digestate from anaerobic digesters without magnet (a), with weak magnet (b), moderate magnet (c), and strong magnets (d) at ambient temperature. The major peaks have been identified as mackinawite (M) and greigite (G).

2022). Moreover, compared to mackinawite, greigite is more magnetic (Lan and Butler, 2014). An increase in greigite crystal in the solid content of the reactors with magnets can have two possible explanations; first, the magnets may concentrate the iron sulfides (especially greigite) in the solid portion, and second, applying a magnetic field may reduce the kinetic resistance (speeds up the transformation) in the mackinawite-greigite transformation. The second possible phenomenon becomes even more critical considering the slow transformation of mackinawite to greigite (Duverger et al., 2020; Hunger and Benning, 2007; Picard et al., 2018). The presence and development of the conductive and magnetic elements in the system, as indicated in XRD analysis of the solid samples, may suggest that more nano-conductive elements are available to be used by different organisms for initiating DIET. However, the role of magnetic field and the surface characters are not clear and need to be investigated further.

3.4. Genetic analysis of microbial culture

DNA extraction and sequencing library preparation was successful for all the samples and yielded between 21,039 and 42,845 DNA reads after quality control of extracted DNA and bioinformatic processing (Fig. 5). As presented in Fig. 5 in all the samples, bacteria genes

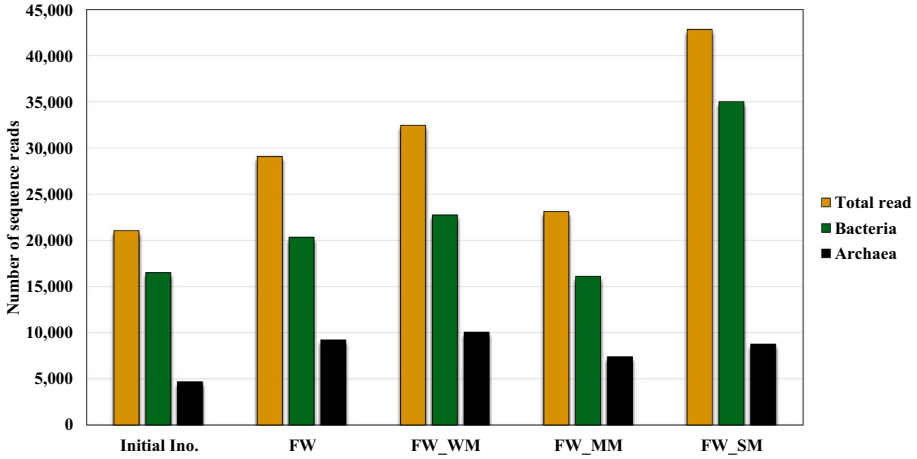

Fig. 5. Sequencing of samples. Total number of sequences (yellow), number of filters reads for bacteria (green) and archaea (black). (For interpretation of the references to colour in this figure legend, the reader is referred to the web version of this article.)

represented around 69.9–81.7 % of all the filter reads, and archaea represented 20.3–30.1 % of the filter reads.

3.4.1. Relative abundance analysis of Archaea and bacteria

Samples from the reactors were taken at the beginning (first day) and the end of the experiment (day 65) to investigate the variation of the microbial community due to applying magnetic fields. Relative sequence fractions of the 14 most abundant bacteria phyla (>0.1 %) within the digesters with/without magnet and initial inoculum libraries produced from Illumina MiSeq sequencing have been provided in Table 4. Table 4 also contains information regarding the most abundant methane-producing genus in the experiments. *Firmicutes* (71.7 %), *Synergistota* (9.7 %), *Proteobacteria* (4.6 %), *Bacteroidota* (7.23 %), and *Caldatribacteriota* (2.5 %) constituent over 95 % of the bacteria in the initial inoculum. After 60 days of experiments and applying a magnetic field, the bacterial community gradually changed. Since this work aimed to investigate the effect of magnetic fields on the microbial community, the focus is here on the samples with magnets. In experiments with WM, MM, and SM, relative abundance (RA) of the Firmicutes increased from 71.7 % to 83.8, 84.8, and 78.11 %, respectively. *Cloacimonadota* species had a similar trend after applying a magnetic field. RA of *Cloacimonadota* increased in WM, MM, and SM to 2.58, 3.86, and 8.97 %, respectively. At the same time, RA of *Synergistota*, *Bacteroidota*, and *Proteobacteria* was reduced as a function of an increase in magnetic field strength. The methanogenesis archaea genus in initial samples belonged to *Methanobacterium* (91.3 %), *Methanoculleus* (7.9 %), *Methanosarcina* (0.7 %), and *Methanobrevibacter* (0.1 %). The magnetic field increased the RA of *Methanosarcina* (8.5 %), and a substantial decrease in the RA of *Methanobacterium* (87.2 %) in the samples was observed.

3.4.2. Effect of magnetic field on the composition of methane producing archaea

Hydrogenotrophic methanogens were the most dominant genus in the initial inoculum, with 99.3 % of the total Archaea community; however, increasing the magnetic field, the RA of *Methanosarcina* (acetoclastic methanogens that can also consume hydrogen or electrons in DIET) increased by up to 12-fold. The high RA of hydrogenotrophic methanogens indicates acetate oxidation, CO_2 oxidation with hydrogen and/or electron and hydrogen conversion to methane were the most likely pathway to generate methane in the initial inoculum. Protein-rich substrates can increase the free nitrogen concentration in the system (Yenigün and Demirel, 2013). Acetoclastic methanogens have lover specific methanogenic activity in elevated ammonia concentration than hydrogenotrophic methanogens (Jiang et al., 2019). Some of the acetoclastic methanogens (e.g., *Methanosaetaceae*) are very sensitive to the ammonia concentration. They cannot tolerate the ammonia nitrogen concentration of over 1 g/L blocking the acetoclastic methanogenesis pathway (Jiang et al., 2019). A lower RA of acetoclastic methanogens in the initial inoculum may suggest that a high total ammonia nitrogen concentration in the samples (2.3 ± 0.2 g/L) could shift the methane production pathway toward hydrogenotrophic methanogenesis rather than acetoclastic. In the samples with magnetic fields, the RA of archaea significantly changed. In experiments with SM, the RA of *Methanosarcina* (8.5 %) increased. At the same time, the RA of *Methanobacterium* (87.2 %) and *Methanoculleus* (4.3 %) reduced. *Methanoculleus* is a hydrogenotrophic organism that can be a partner of syntrophic acetate-oxidizing bacteria (Mosbæk et al., 2016); however, it should be noted that the abundance of *Methanoculleus* and *Methanobacterium* was reduced while the abundance of *Methanosarcina* in the experiments including magnets was raised. *Methanosarcina* are multifunction microorganisms that can consume either hydrogen or acetate to produce methane (Zhang et al., 2019). It is also well-known that the *Methanosarcina* class is capable of transferring electron in a DIET metabolism in AD (Holmes et al., 2021). *Methanosarcina* in the presence of syntrophic partner can potentially take over the role of the *Methanoculleus* and produce methane from hydrogen or electrons (Mosbæk et al., 2016). An increase in the population of *Methanosarcina* sp. as a function of an increase in the magnetic field and methane production yield in high ammonia concentration can be potentially linked to stimulation of DIET between syntrophic microorganisms; however, DIET among syntrophic partners deserves further pure coculture investigations.

Table 4
Relative sequence fraction of the 14 most abundant bacteria phyla and 4 most abundant archaea genes (>0.01 %) within the digesters with/without magnet and initial inoculum libraries produced from Illumina MiSeq sequencing of Bacteria and Archaea 16S rRNA gene amplicons. The red colors represent the data bars for each species.

	Initial ino.	FW	FW_WM	FW_MM	FW_SM
Bacteria phylum					
Actinobacteriota	0.39	0.25	0.27	0.21	0.20
Bacteroidota	7.23	4.50	2.91	2.33	3.44
Caldatribacteriota	2.53	2.92	2.57	2.88	2.21
Chloroflexi	0.06	0.29	0.20	0.28	0.45
Cloacimonadota	1.72	3.51	2.58	3.86	8.97
Desulfobacterota	0.04	0.06	0.06	0.08	0.06
Firmicutes	71.71	81.42	83.80	84.79	78.11
Planctomycetota	0.00	0.04	0.02	0.03	0.04
Proteobacteria	4.60	2.36	2.64	2.12	3.06
Spirochaetota	0.01	0.03	0.01	0.00	0.02
Synergistota	9.73	3.42	3.92	2.52	2.78
Verrucomicrobiota	0.32	0.14	0.08	0.15	0.06
WPS-2	0.10	0.20	0.12	0.13	0.07
Uncultured	1.56	0.84	0.82	0.63	0.54
Archaea genes					
Methanobacterium	91.3	93.1	94.8	93.4	87.2
Methanobrevibacter	0.1	0.0	0.0	0.0	0.0
Methanoculleus	7.9	5.6	3.8	2.7	4.3
Methanosarcina	0.7	1.3	1.4	3.8	8.5

3.4.3. Variations in bacterial community structure and possible DIET pathways

RA of different families in the bacterial community with the highest fluctuation is presented in Table 5. Since the bacterial community in most of the samples was relatively stable, the most fluctuating families within bacteria are of interest. A specific focus is given to those families with an upward trend increase in RA as a function of growth in the magnetic field. RA of different family members of several species, including *Firmicutes*, *Chloroflexi*, *Proteobacteria*, *Cloacimonadota* and *Desulfobacterota*, showed an increase with the magnet field strength. RA of *Sedimentibacteraceae*, *Erysipelatoclostridiaceae*, *Anaerolineaceae* and *Pseudomonadaceae* showed the highest increase by up to 100-, 16-, 9.4, and 9.05-fold after increasing the magnetic field to over 180 T. The RA of W27, *Lactobacillaceae*, *Guggenheimella*, *Lutispora*, *Proteiniboraceae*, *Desulfomicrobiaceae*, *Dethiobacteraceae*, and *Syntrophomonadaceae* were increased by over 2-fold.

Some members of *Sedimentibacteraceae* are capable of reducing iron (Zhao et al., 2021). Zhao et al. have shown that family members of *Sedimentibacteraceae* contain genera for pilA making them potential candidates for direct electron transfer to *electrophic* methanogens (e.g., *Methanothrix* and *Methanosarcina*) (Feng et al., 2022; Zhao et al., 2020). Genera belonging to *Erysipelatoclostridiaceae* families are anaerobic fermenters, degrading carbohydrates to generate lactose, hydrogen, acetate, butyrate and propionate (Palomo-Briones et al., 2022; Treu et al., 2019; Yutin and Galperin, 2013). *Anaerolineaceae*, as a family within *Chloroflexi* phylum, are widespread in AD reactors utilizing the carbohydrates and proteinaceous carbons under AD (McIlroy et al., 2017). Nakasaki et al. and Yamada et al. have reported that the *Anaerolineaceae* are dominant in lipid-rich ADs, which is relevant to the nature of the substrate used in this study (Nakasaki et al., 2019; Yamada et al., 2006). It is reported in previous research studies that *Anaerolineaceae* are syntrophic partners of methanogens for methane productions (Azman et al., 2017; De Vrieze et al., 2015). It is also reported by Wang et al. that the

Table 5
Heat map of the 34 most abundance bacterial families (>0.01 %). Relative abundance (RA) of the 35 most fluctuating families within the bacteria (heat map) and the normalized values of RA of the families in different samples-per RA of corresponding families in the initial inoculum (right). Families are listed from the largest reduction to largest growth in R. A. ratio of FE_SM experiments.

Phylum	Family	Initial Ino.	FW	FW _WM	FW _MM	FW _SM	(R. A. of Families) $_{samples}$ / (R. A. of Families) $_{Initial\ Ino.}$		
							FW _WM	FW _MM	FW _SM
Blank		2.44	0.79	0.82	0.65	0.46	0.34	0.27	0.19
Firmicutes	Limnochordaceae	0.10	0.07	0.05	0.01	0.02	0.50	0.10	0.20
Firmicutes	Tepidanaerobacter	0.14	0.02	0.04	0.03	0.04	0.29	0.21	0.29
Firmicutes	Peptostreptococcaceae	0.21	0.06	0.03	0.03	0.07	0.14	0.14	0.33
Proteobacteria	Alcaligenaceae	4.23	2.21	2.21	1.37	1.39	0.52	0.32	0.33
Proteobacteria	Xanthobacteraceae	0.04	0.00	0.00	0.01	0.02	0.00	0.25	0.50
Synergistota	Synergistaceae	9.73	3.42	3.92	2.52	3.57	0.40	0.26	0.37
Bacteroidota	Lentimicrobiaceae	4.61	2.71	1.30	1.16	1.83	0.28	0.25	0.40
Firmicutes	midas_f	34.25	30.87	31.35	29.00	15.53	0.92	0.85	0.45
Bacteroidota	Dysgonomonadaceae	2.17	1.42	1.26	0.85	1.26	0.58	0.39	0.58
Proteobacteria	Rhodobacteraceae	0.03	0.03	0.00	0.00	0.02	0.00	0.00	0.67
WPS-2	midas_f_1770	0.10	0.20	0.12	0.12	0.08	1.20	1.20	0.80
Bacteroidota	Marinilabiliaceae	0.04	0.03	0.06	0.05	0.03	1.50	1.25	0.75
Desulfobacterota	Desulfobulbus	0.01	0.01	0.02	0.03	0.01	2.00	3.00	1.00
Firmicutes	Caldicoprobacteraceae	0.20	0.10	0.10	0.04	0.17	0.50	0.20	0.85
Firmicutes	Christensenellaceae	0.80	0.82	0.33	0.47	0.68	0.41	0.59	0.85
Caldatribacteriota	Caldatribacteriaceae	2.53	2.92	2.57	2.88	2.34	1.02	1.14	0.92
Firmicutes	Anaerovoracaceae	0.07	0.24	0.35	0.35	0.30	1.30	1.30	1.11
Actinobacteriota	Corynebacteriaceae	0.16	0.22	0.22	0.16	0.18	1.38	1.00	1.13
Bacteroidota	Rikenellaceae	0.34	0.26	0.21	0.20	0.39	0.62	0.59	1.15
Firmicutes	Hungateiclostridiaceae	9.82	13.23	13.44	15.68	15.49	1.37	1.60	1.58
Firmicutes	Family_XI	6.93	9.66	9.96	10.18	11.06	1.44	1.47	1.60
Firmicutes	Syntrophomonadaceae	1.79	1.68	2.50	2.67	3.58	1.40	1.49	2.00
Firmicutes	Dethiobacteraceae	6.26	5.97	8.49	9.73	12.88	1.36	1.55	2.06
Desulfobacterota	Desulfomicrobiaceae	0.02	0.02	0.04	0.04	0.05	2.00	2.00	2.50
Firmicutes	Proteiniboraceae	1.99	3.55	1.84	1.41	5.23	0.92	0.71	2.63
Firmicutes	Lutispora	0.08	0.18	0.27	0.18	0.24	3.38	2.25	3.00
Firmicutes	Guggenheimella	3.97	5.13	11.42	11.82	12.59	2.88	2.98	3.17
Firmicutes	Lactobacillaceae	0.63	2.10	2.04	1.95	2.36	3.24	3.10	3.75
Cloacimonadota	W27	1.72	3.37	2.59	4.02	7.05	1.51	2.34	4.10
Proteobacteria	Pseudomonadaceae	0.19	0.11	0.40	0.56	1.72	2.11	2.95	9.05
Chloroflexi	Anaerolineaceae	0.05	0.03	0.30	0.28	0.47	6.00	5.60	9.40
Firmicutes	Erysipelatoclostridiaceae	0.01	0.02	0.08	0.08	0.16	8.00	8.00	16.00
Firmicutes	Sedimentibacteraceae	0.00	0.05	0.06	0.08	0.10	60.00	80.00	100.00

Anaerolineaceae can potentially contribute to DIET in presence of conductive materials in the digesters (G. Wang et al., 2018). The results of this study suggest that that magnetic field may enhance the electron transfer process among methanogens and *Anaerolineaceae* resulting in an increase in RA of *Anaerolineaceae* as a function of magnetic field (Xia et al., 2016). Genus belonging to *Pseudomonadaceae*, including *Pseudomonas*, were reported as electrogenic bacteria responsible for converting VFAs to electric current in microbial fuel cells (Freguia et al., 2010). Moreover, family members of *Pseudomonadaceae* can convert alcohols to acetate and electrons. These electrons can be further transferred to *Methanosarcina* through DIET. However, the *Pseudomonadaceae* are not sufficient alone for the electron transfer from central metabolism to cell surface (Lovley, 2006) and a conductive element is required to initiated DIET (Y. Li et al., 2022; Liu et al., 2012). Results from XRD analyses indicated that the magnetic and conductive materials were concentrated in the digesters exposed to magnetic fields. Presence of these conductive elements in experiments with magnet can potentially initiate DIET among *Pseudomonadaceae* and methane producing archaea including *Methanobacterium* and *Methanosarcina* (Lin et al., 2017; Qi et al., 2021; Wan et al., 2021).

W27, a family within *Cloacimonadota* phylum, are reported as active bacteria in the degradation of long-chain fatty acids (LCFA) in lipid-rich substrates through a cyclic β-oxidation (Shakeri Yekta et al., 2019). Cleavage of LCFA through cyclic β-oxidation resulting in acetate, hydrogen and/or formate (Perman et al., 2022). *Lactobacillaceae* is also characterized as hydrolyzing bacteria converting simple and complex sugars to acetate, ethanol, CO_2, formate, or succinate (Felis and Pot, 2014; Lourinho et al., 2020; Poszytek et al., 2017). Studies have shown that magnetic fields can influence the metal ions and intracellular enzymes. Cell membrane and electron transport systems can be affected by electrodynamic interaction between living organisms' electric current and magnetic force (Hu et al., 2020; Zhang et al., 2015; Zieliński et al., 2021). An increased RA of W27 and *Lactobacillaceae* in experiments with magnet can potentially be linked to an improved hydrolytic consortium; however, the results here are not sufficient for such a conclusion and an advanced meta-omic-based technique needs to be employed to investigate the enzymes involved in the process. The protein content of FW results in an elevated ammonia concentration in the system. *Guggenheimella* is detected as anaerobic fermenters converting carbohydrates to butyrate, propionate, and acetate, participating in syntrophic oxidation under ammonia stress (Mathai et al., 2020; Zhang et al., 2022). *Lutispora* belonging to the *Firmicutes* phylum have been reported as key degrader of proteinaceous substrates (Chen et al., 2018). The end products from these microorganisms in anaerobic fermentation at 40 °C are acetate, isobutyrate, propionate and isovalerate (Jiang et al., 2020; Pervin et al., 2013; Shiratori et al., 2008). Bai et al. have observed a close partnership among *Lutispora* and methane producing archaea with high VFA and protein content digesters (Bai et al., 2019). Even though RA of *Lutispora* is relatively low in this system, it potentially plays an important role in AD of FW (Jiang et al., 2022). Like *Lutispora*, members of *Proteiniboraceae* family including *Proteiniborus* are protein-specific utilizing bacteria under elevated ammonia concentrations (Chen et al., 2018; Dai et al., 2016). The *Proteiniborus* is gram negative mesophilic anaerobic fermenter that converts proteins to acetic acid, hydrogen, ethanol, carbon dioxide (Dai et al., 2016; Niu et al., 2008). Cao et al. demonstrated that the *Proteiniborus* have significant role in sustaining hydrogen consuming methanogens (Cao et al., 2022). An increase in RA of protein degraders after applying magnetic field may suggest that the proposed approach can positively influence the degradation of proteins.

Even though *Desulfomicrobiaceae* have shown a relatively lower presence in all the experiments, the increased RA of genus belonging to *Desulfomicrobiaceae* is of interest. *Desulfomicrobium* (listed in the supplementary document), a family member of *Desulfomicrobiaceae*, are incomplete oxidizing sulfate-reducing bacteria (IO-SRB) capable of degrading organic carbons to acetate (Xing et al., 2020). The electron donors for IO-SBR are pyruvate, lactate, methanol, ethanol, and glycerol using sulfate as an electron acceptor (Lu et al., 2017; S. Wang et al., 2021). Unlike complete oxidizing sulfate-reducing bacteria (CO-SRB) that compete with methane-producing archaea for H_2 and acetate utilization, IO-SRB cooperate with methanogens (Wu et al., 2018). Several researchers have reported that adding iron containing materials (e.g., ferroferric oxide (Fe3O4), magnetite, nanoscale zero valent iron) can improve the cooperation between IC-SRB and methanogens while reducing H_2S concentration the reactors (Amen et al., 2018; Liu et al., 2019; Z. Wang et al., 2021). Xing et al. have shown that genus belonging to *Desulfomicrobiaceae* and methane-producing archaea can potentially contribute in methane production by DIET in presence of iron-based conductive materials (Xing et al., 2020). Increased RA of *Desulfomicrobiaceae* after adding $FeCl_3$ and applying a magnetic field in this study may suggest that a DIET can potentially accrue among *Desulfomicrobiaceae* and methane-producing archaea. *Dethiobacteraceae* are also suggested as syntrophic acetate oxidizing bacteria in high ammonia content (Dyksma et al., 2020; Perman et al., 2022; Trutschel et al., 2022). Dyksma et al. have suggested that the members of *Dethiobacteraceae* family express genes encoding ferredoxin which is crucial for methane production through carbon dioxide oxidation pathway (Dyksma et al., 2020). It is also argued that these genes are essential for electron uptake by *Methanosarcina* during DIET (Holmes et al., 2018, 2021; Wagner et al., 2017). Increased RA of *Methanosarcina* and *Dethiobacteraceae* as a function of elevated magnetic field in this study might be related to an improved electron transfer process through iron-sulfide proteins and close partnership among SAO-based *Dethiobacteraceae* and *Methanosarcina*; however, this hypothesis requires stronger supports through detailed analysis of gene expression. *Syntrophomonadaceae* are active butyrate-reducing bacteria through hydrogen interspecies transfer pathway in close association with hydrogen consumers in AD (Zhao et al., 2016). Presence of *Syntrophomonadaceae* is crucial to maintain the VFA degradation and methane production in the system (Li et al., 2015; Zhang et al., 2020).

A simultaneous increase in RA of the *Methanosarcina* and several potential DIET-active bacteria families (e.g., *Sedimentibacteraceae*, *Anaerolineaceae*, *Pseudomonadaceae*, and *Desulfomicrobiaceae*) may suggest that DIET would be an alternative pathway for biomethane production in systems including magnetic field after adding $FeCl_3$. The microbial community structure was less diverse in all the samples than in samples from other anoxic environments, mainly due to harsh conditions (such as high ammonia content) developed during AD of FW. It is worth mentioning that, due to the H_2S management strategies in the plant from which the initial inoculum originated, the initial inoculum contained some conductive elements, including mackinawite and greigite. The presence of hydrogenotrophic methanogens and enriched Firmicutes bacteria may indicate that DIET could be an important pathway for methane production; however, applying an external magnetic field could significantly increase methane production potentially due to an improved syntrophic partnership among different bacteria and archaea.

This study indicates that increasing magnetic field strength may increase the biogas production. These substances (e.g., ferredoxin) could be responsible for enzymatic effects as well as stimulating DIET in the system, and it is therefore suggested that the enzyme analysis be carried out and combined with magnetic stimulation to search for possible synergies.

The magnetic separation and recycling will selectively recycle magnetic material, and the electron donors and recipients that interact with the magnetic/conducting surfaces. This could therefore be an efficient way forward in separating hydraulic residence time in the reactor from the residence time of the microorganisms. Therefore, magnetic separation and recirculation of iron sulfide crystals may turn stirred tank biogas reactors into highly efficient reactors for biogas production.

4. Conclusion

Protein- and fat-rich FW was employed as a feedstock for AD. To prevent H_2S generation from the protein, $FeCl_3$ was added to the system. Conductive and magnetic elements, including mackinawite and greigite, were generated during AD. Microorganisms may use these elements as a surface for developing biofilm and facilitating the DIET. A magnetic field in the system increased methane production yield and concentrated conductive materials while reducing the H_2S content. The genetic analysis revealed that the magnetic field changed the structure of the microbial community toward a fat-hydrolysis-rich culture. Magnetic fields could potentially stimulate DIET.

CRediT authorship contribution statement

S. B. H.: conceptualization, reactor design, methodology, formal analysis, investigation, writing – Original Draft. **S. J. H.**: scientific discussion, review & editing. **J. J. L.**: supervision, validation, review & editing. **K. M. L.**: supervision, validation, conceptualization, review and editing.

Declaration of competing interest

The authors declare the following financial interests/personal relationships which may be considered as potential competing interests: Seyedbehnam Hashemi reports financial support, administrative support, article publishing charges, equipment, drugs, or supplies, travel, and writing assistance were provided by Norwegian University of Science and Technology. Svein Jarle Horn reports financial support and writing assistance were provided by Norwegian University of Life Sciences. Jacob J. Lamb reports statistical analysis and writing assistance were provided by Norwegian University of Science and Technology. Kristian M. Lien reports administrative support, equipment, drugs, or supplies, and writing assistance were provided by Norwegian University of Science and Technology. Seyedbehnam Hashemi reports a relationship with ENERSENSE strategic research program initiative that includes: funding grants and travel reimbursement. One of the co-authors works at the Norwegian institute for bioeconomy research (NIBIO).

Data availability

Data will be made available on request.

Acknowledgements

The authors acknowledge the financial support from Norwegian University of Science and Technology (NTNU) and Norwegian Research Council through ENERSENSE strategic research program initiative.

References

Aas, T.S., 2016. A preliminary test of the possibility for reclamation of phosphorus from aquaculture sludge. A CtrlAQUA pre-project - Nofima [WWW Document]. URL. Nofirma (accessed 5.24.22). https://nofima.no/publikasjon/1344766/.

Ahuja, I., Dauksas, E., Remme, J.F., Richardsen, R., Løes, A.K., 2020. Fish and fish waste-based fertilizers in organic farming – with status in Norway: a review. Waste Manag. 115, 95–112. https://doi.org/10.1016/J.WASMAN.2020.07.025.

Albertsen, M., Karst, S.M., Ziegler, A.S., Kirkegaard, R.H., Nielsen, P.H., 2015. Back to basics – the influence of DNA extraction and primer choice on phylogenetic analysis of activated sludge communities. PLoS One 10, e0132783. https://doi.org/10.1371/JOURNAL.PONE.0132783.

Amen, T.W.M., Eljamal, O., Khalil, A.M.E., Matsunaga, N., 2018. Evaluation of sulfate-containing sludge stabilization and the alleviation of methanogenesis inhibitation at mesophilic temperature. J. Water Process Eng. 25, 212–221. https://doi.org/10.1016/J.JWPE.2018.08.004.

Apprill, A., McNally, S., Parsons, R., Weber, L., 2015. Minor revision to V4 region SSU rRNA 806R gene primer greatly increases detection of SAR11 bacterioplankton. Aquat. Microb. Ecol. 75, 129–137.

Azman, S., Khadem, A.F., Plugge, C.M., Stams, A.J.M., Bec, S., Zeeman, G., 2017. Effect of humic acid on anaerobic digestion of cellulose and xylan in completely stirred tank reactors: inhibitory effect, mitigation of the inhibition and the dynamics of the microbial communities. Appl. Microbiol. Biotechnol. 101, 889–901.

Baek, G., Kim, J., Lee, C., 2019. A review of the effects of iron compounds on methanogenesis in anaerobic environments. Renew. Sustain. Energy Rev. https://doi.org/10.1016/j.rser.2019.109282.

Bai, Y., Xu, R., Wang, Q.P., Zhang, Y.R., Yang, Z.H., 2019. Sludge anaerobic digestion with high concentrations of tetracyclines and sulfonamides: dynamics of microbial communities and change of antibiotic resistance genes. Bioresour. Technol. 276, 51–59. https://doi.org/10.1016/J.BIORTECH.2018.12.066.

Barua, S., Dhar, B.R., 2017. Advances towards understanding and engineering direct interspecies electron transfer in anaerobic digestion. Bioresour. Technol. 244, 698–707. https://doi.org/10.1016/J.BIORTECH.2017.08.023.

Buckel, W., Thauer, R.K., 2018. Flavin-based electron bifurcation, ferredoxin, flavodoxin, and anaerobic respiration with protons (Ech) or NAD + (Rnf) as electron acceptors: a historical review. Front. Microbiol. 9 https://doi.org/10.3389/FMICB.2018.00401.

Cai, Y., Zheng, Z., Wang, X., 2021. Obstacles faced by methanogenic archaea originating from substrate-driven toxicants in anaerobic digestion. J. Hazard. Mater. 403, 123938 https://doi.org/10.1016/j.jhazmat.2020.123938.

Cao, H., Sun, J., Wang, K., Zhu, G., Li, X., Lv, Y., Wang, Z., Feng, Q., Feng, J., 2022. Performance of bioelectrode based on different carbon materials in bioelectrochemical anaerobic digestion for methanation of maize straw. Sci. Total Environ. 832, 154997 https://doi.org/10.1016/J.SCITOTENV.2022.154997.

Chang, L., Roberts, A.P., Tang, Y., Rainford, B.D., Muxworthy, A.R., Chen, Q., 2008. Fundamental magnetic parameters from pure synthetic greigite (Fe3S4). J. Geophys. Res. Solid Earth 113, 6104. https://doi.org/10.1029/2007JB005502.

Chang, Y.S., Savitha, S., Sadhasivam, S., Hsu, C.K., Lin, F.H., 2011. Fabrication, characterization, and application of greigite nanoparticles for cancer hyperthermia. J. Colloid Interface Sci. 363, 314–319. https://doi.org/10.1016/J.JCIS.2010.06.069.

Chen, S., He, J., Wang, H., Dong, B., Li, N., Dai, X., 2018. Microbial responses and metabolic pathways reveal the recovery mechanism of an anaerobic digestion system subjected to progressive inhibition by ammonia. Chem. Eng. J. 350, 312–323. https://doi.org/10.1016/J.CEJ.2018.05.168.

Chen, Y., Xue, Q., Liu, L., Kong, Y., He, X., Ma, J., Ge, S., Yuan, Z., 2019. Influences of magnetic powder addition on the anaerobic digestion of municipal dewatered sludge. Environ. Prog. Sustain. Energy 38, 374–379.

Choong, Y.Y., Norli, I., Abdullah, A.Z., Yhaya, M.F., 2016. Impacts of trace element supplementation on the performance of anaerobic digestion process: a critical review. Bioresour. Technol. 209, 369–379. https://doi.org/10.1016/J.BIORTECH.2016.03.028.

Dai, X., Yan, H., Li, N., He, J., Ding, Y., Dai, L., Dong, B., 2016. Metabolic adaptation of microbial communities to ammonium stress in a high solid anaerobic digester with dewatered sludge. Sci. Rep. 6, 1–10. https://doi.org/10.1038/srep28193.

De Vrieze, J., Gildemyn, S., Vilchez-Vargas, R., Jáuregui, R., Pieper, D.H., Verstraete, W., Boon, N., 2015. Inoculum selection is crucial to ensure operational stability in anaerobic digestion. Appl. Microbiol. Biotechnol. 99, 189–199.

Dubé, C.D., Guiot, S.R., 2015. Direct interspecies electron transfer in anaerobic digestion: a review. Biogas Sci. Technol. 101–115. https://doi.org/10.1007/978-3-319-21993-6_4/FIGURES/1.

Duverger, A., Berg, J.S., Busigny, V., Guyot, F., Bernard, S., Miot, J., 2020. Mechanisms of pyrite formation promoted by sulfate-reducing bacteria in pure culture. Front. Earth Sci. 8, 457. https://doi.org/10.3389/FEART.2020.588310/BIBTEX.

Dyksma, S., Jansen, L., Gallert, C., 2020. Syntrophic acetate oxidation replaces acetoclastic methanogenesis during thermophilic digestion of biowaste. Microbiome 8, 1–14. https://doi.org/10.1186/S40168-020-00862-5/FIGURES/5.

Erdirencelebi, D., Kucukhemek, M., 2018. Control of hydrogen sulphide in full-scale anaerobic digesters using iron (III) chloride: performance, origin and effects. Water SA 44, 176–183. https://doi.org/10.4314/WSA.V44I2.04.

Felis, G.E., Pot, B., 2014. The family Lactobacillaceae. Lact. Acid Bact. Biodivers. Taxon. 9781444333831, 245–247. https://doi.org/10.1002/9781118655252.PART4.

Feng, D., Xia, A., Huang, Y., Zhu, Xianqing, Zhu, Xun, Liao, Q., 2022. Effects of carbon cloth on anaerobic digestion of high concentration organic wastewater under various mixing conditions. J. Hazard. Mater. 423, 127100 https://doi.org/10.1016/J.JHAZMAT.2021.127100.

Fotidis, I.A., Karakashev, D., Kotsopoulos, T.A., Martzopoulos, G.G., Angelidaki, I., 2013. Effect of ammonium and acetate on methanogenic pathway and methanogenic community composition. FEMS Microbiol. Ecol. 83, 38–48. https://doi.org/10.1111/J.1574-6941.2012.01456.X.

Frank, J.A., Arntzen, M.Ø., Sun, L., Hagen, L.H., McHardy, A.C., Horn, S.J., Eijsink, V.G. H., Schnürer, A., Pope, P.B., 2016. Novel syntrophic populations dominate an ammonia-tolerant methanogenic microbiome. Msystems 1, e00092-16.

Freguia, S., Teh, E.H., Boon, N., Leung, K.M., Keller, J., Rabaey, K., 2010. Microbial fuel cells operating on mixed fatty acids. Bioresour. Technol. 101, 1233–1238.

Gallegos, T.J., Sung, P.H., Hayes, K.F., 2007. Spectroscopic investigation of the uptake of arsenite from solution by synthetic mackinawite. Environ. Sci. Technol. 41, 7781–7786. https://doi.org/10.1021/ES070613C/SUPPL_FILE/ES070613CSI20070820_083650.PDF.

Gramp, J.P., Bigham, J.M., Jones, F.S., Tuovinen, O.H., 2010. Formation of Fe-sulfides in cultures of sulfate-reducing bacteria. J. Hazard. Mater. 175, 1062–1067. https://doi.org/10.1016/J.JHAZMAT.2009.10.119.

Hashemi, B., Sarker, S., Lamb, J.J., Lien, K.M., 2021. Yield improvements in anaerobic digestion of lignocellulosic feedstocks. J. Clean. Prod. https://doi.org/10.1016/j.jclepro.2020.125447.

Hashemi, S., Hashemi, S.E., Lien, K.M., Lamb, J.J., 2021. Molecular microbial community analysis as an analysis tool for optimal biogas production. Microorganisms 9, 1162. https://doi.org/10.3390/MICROORGANISMS9061162.

Hellman, J., Ek, A., Sundberg, C., Johansson, M., Svensson, B., Karlsson, M., 2010. Mechanisms of increased methane production through re-circulation of magnetic biomass carriers in an experimental continuously stirred tank reactor. In: 12th World Congress on Anaerobic Digestion (AD12). Oct 31st-Nov 4th, 2010. IWA Publishing, Guadalajara, Mexico.

Holmes, D.E., Rotaru, A.E., Ueki, T., Shrestha, P.M., Ferry, J.G., Lovley, D.R., 2018. Electron and proton flux for carbon dioxide reduction in methanosarcina barkeri during direct interspecies electron transfer. Front. Microbiol. 9, 3109. https://doi.org/10.3389/FMICB.2018.03109/BIBTEX.

Holmes, D.E., Zhou, J., Ueki, T., Woodard, T., Lovley, D.R., 2021. Mechanisms for electron uptake by Methanosarcina acetivorans during direct interspecies electron transfer. MBio 12. https://doi.org/10.1128/MBIO.02344-21/SUPPL_FILE/MBIO.02344-21-ST005.DOCX.

Hu, B., Wang, Y., Quan, J., Huang, K., Gu, X., Zhu, J., Yan, Y., Wu, P., Yang, L., Zhao, J., 2020. Effects of static magnetic field on the performances of anoxic/oxic sequencing batch reactor. Bioresour. Technol. 309, 123299.

Hunger, S., Benning, L.G., 2007. Greigite: a true intermediate on the polysulfide pathway to pyrite. Geochem. Trans. 8, 1–20. https://doi.org/10.1186/1467-4866-8-1/FIGURES/9.

Jeong, H.Y., Lee, J.H., Hayes, K.F., 2008. Characterization of synthetic nanocrystalline mackinawite: crystal structure, particle size, and specific surface area. Geochim. Cosmochim. Acta 72, 493–505. https://doi.org/10.1016/J.GCA.2007.11.008.

Jiang, Y., McAdam, E., Zhang, Y., Heaven, S., Banks, C., Longhurst, P., 2019. Ammonia inhibition and toxicity in anaerobic digestion: a critical review. J. Water Process Eng. 32, 100899 https://doi.org/10.1016/J.JWPE.2019.100899.

Jiang, J., Wu, P., Sun, Y., Guo, Y., Song, B., Huang, Y., Xing, T., Li, L., 2020. Comparison of microbial communities during anaerobic digestion of kitchen waste: effect of substrate sources and temperatures. Bioresour. Technol. 317, 124016 https://doi.org/10.1016/J.BIORTECH.2020.124016.

Jiang, X., Lyu, Q., Bi, L., Liu, Y., Xie, Y., Ji, G., Huan, C., Xu, L., Yan, Z., 2022. Improvement of sewage sludge anaerobic digestion through synergistic effect combined trace elements enhancer with enzyme pretreatment and microbial community response. Chemosphere 286, 131356. https://doi.org/10.1016/J.CHEMOSPHERE.2021.131356.

Jin, Z., Zhao, Z., Zhang, Y., 2019. Potential of direct interspecies electron transfer in synergetic enhancement of methanogenesis and sulfate removal in an up-flow anaerobic sludge blanket reactor with magnetite. Sci. Total Environ. 677, 299–306. https://doi.org/10.1016/J.SCITOTENV.2019.04.372.

Kadota, P., Markin, P., Eskicioglu, C., 2019. US11274054B2 - Syntrophic enrichment for enhanced digestion process. Google Patents.

Kato, S., Hashimoto, K., Watanabe, K., 2012. Methanogenesis facilitated by electric syntrophy via (semi) conductive iron-oxide minerals. Environ. Microbiol. 14, 1646–1654.

Kumar, V., Nabaterega, R., Khoei, S., Eskicioglu, C., 2021. Insight into interactions between syntrophic bacteria and archaea in anaerobic digestion amended with conductive materials. Renew. Sustain. Energy Rev. https://doi.org/10.1016/j.rser.2021.110965.

Lamb, J.J., Hohmann-Marriott, M.F., 2017. Manganese acquisition is facilitated by PilA in the cyanobacterium Synechocystis sp. PCC 6803. PLoS One 12.

Lamb, J.J., Hill, R.E., Eaton-Rye, J.J., Hohmann-Marriott, M.F., 2014. Functional role of PilA in iron acquisition in the cyanobacterium Synechocystis sp. PCC 6803. PLoS One 9.

Lan, Y., Butler, E.C., 2014. Monitoring the transformation of mackinawite to greigite and pyrite on polymer supports. Appl. Geochem. 50, 1–6. https://doi.org/10.1016/J.APGEOCHEM.2014.07.020.

Li, H., Chang, J., Liu, P., Fu, L., Ding, D., Lu, Y., 2015. Direct interspecies electron transfer accelerates syntrophic oxidation of butyrate in paddy soil enrichments. Environ. Microbiol. 17, 1533–1547. https://doi.org/10.1111/1462-2920.12576/SUPPINFO.

Li, Y., Chen, Y., Wu, J., 2019. Enhancement of methane production in anaerobic digestion process: a review. Appl. Energy 240, 120–137. https://doi.org/10.1016/J.APENERGY.2019.01.243.

Li, L., Liu, H., Chen, Y., Yang, D., Cai, C., Yuan, S., Dai, X., 2022. Effect of Magnet-Fe3O4 composite structure on methane production during anaerobic sludge digestion: establishment of direct interspecies electron transfer. Renew. Energy 188, 52–60. https://doi.org/10.1016/J.RENENE.2022.01.101.

Li, Y., Wang, Z., Jiang, Z., Feng, L., Pan, J., Zhu, M., Ma, C., Jing, Z., Jiang, H., Zhou, H., Sun, H., Liu, H., 2022. Bio-based carbon materials with multiple functional groups and graphene structure to boost methane production from ethanol anaerobic digestion. Bioresour. Technol. 344, 126353 https://doi.org/10.1016/J.BIORTECH.2021.126353.

Lin, R., Cheng, J., Zhang, J., Zhou, J., Cen, K., Murphy, J.D., 2017. Boosting biomethane yield and production rate with graphene: the potential of direct interspecies electron transfer in anaerobic digestion. Bioresour. Technol. 239, 345–352. https://doi.org/10.1016/J.BIORTECH.2017.05.017.

Liu, F., Rotaru, A.E., Shrestha, P.M., Malvankar, N.S., Nevin, K.P., Lovley, D.R., 2012. Promoting direct interspecies electron transfer with activated carbon. Energy Environ. Sci. https://doi.org/10.1039/c2ee22459c.

Liu, Y., Gu, M., Yin, Q., Wu, G., 2019. Inhibition mitigation and ecological mechanism of mesophilic methanogenesis triggered by supplement of ferroferric oxide in sulfate-containing systems. Bioresour. Technol. 288, 121546 https://doi.org/10.1016/J.BIORTECH.2019.121546.

Lourinho, G., Rodrigues, L.F.T.G., Brito, P.S.D., 2020. Recent advances on anaerobic digestion of swine wastewater. Int. J. Environ. Sci. Technol. 17, 4917–4938. https://doi.org/10.1007/S13762-020-02793-Y/TABLES/5.

Lovley, D.R., 2006. Bug juice: harvesting electricity with microorganisms. Nat. Rev. Microbiol. 4, 497–508.

Lovley, D.R., 2022. Electrotrophy: other microbial species, iron, and electrodes as electron donors for microbial respirations. Bioresour. Technol. 345, 126553 https://doi.org/10.1016/J.BIORTECH.2021.126553.

Lu, X., Zhen, G., Ni, J., Kubota, K., Li, Y.Y., 2017. Sulfidogenesis process to strengthen re-granulation for biodegradation of methanolic wastewater and microorganisms evolution in an UASB reactor. Water Res. 108, 137–150. https://doi.org/10.1016/J.WATRES.2016.10.073.

Luo, H., Sun, Y., Taylor, M., Nguyen, C., Strawn, M., Broderick, T., Wang, Z.W., 2022. Impacts of aluminum- and iron-based coagulants on municipal sludge anaerobic digestibility, dewaterability, and odor emission. Water Environ. Res. 94, e1684 https://doi.org/10.1002/WER.1684.

Lv, N., Zhao, L., Wang, R., Ning, J., Pan, X., Li, C., Cai, G., Zhu, G., 2020. Novel strategy for relieving acid accumulation by enriching syntrophic associations of syntrophic fatty acid-oxidation bacteria and H2/formate-scavenging methanogens in anaerobic digestion. Bioresour. Technol. 313, 123702 https://doi.org/10.1016/J.BIORTECH.2020.123702.

Martins, G., Salvador, A.F., Pereira, L., Alves, M.M., 2018. Methane production and conductive materials: a critical review. Environ. Sci. Technol. 52, 10241–10253. https://doi.org/10.1021/ACS.EST.8B01913/ASSET/IMAGES/LARGE/ES-2018-01913F_0003.JPEG.

Masood, S., 2017. Effect of weak magnetic field on bacterial growth. Biophys. Rev. Lett. 12, 177–186.

Mathai, P.P., Nicholes, M.S., Venkiteshwaran, K., Brown, C.M., Morris, R.L., Zitomer, D. H., Maki, J.S., 2020. Dynamic shifts within volatile fatty acid–degrading microbial communities indicate process imbalance in anaerobic digesters. Appl. Microbiol. Biotechnol. 104, 4563–4575. https://doi.org/10.1007/S00253-020-10552-9/FIGURES/4.

McIlroy, S.J., Kirkegaard, R.H., Dueholm, M.S., Fernando, E., Karst, S.M., Albertsen, M., Nielsen, P.H., 2017. Culture-independent analyses reveal novel anaerolineaceae as abundant primary fermenters in anaerobic digesters treating waste activated sludge. Front. Microbiol. 8, 1134. https://doi.org/10.3389/FMICB.2017.01134/BIBTEX.

Metcalf, Eddy, I., Tchobanoglous, G., Stensel, H., Tsuchihashi, R., Burton, F., 2014. Wastewater Engineering: Treatment and Resource Recovery, , 5th intern. ed.Volume 1. McGraw-Hill, New York.

Møller, H.B., Sommer, S.G., Ahring, B.K., 2004. Methane productivity of manure, straw and solid fractions of manure. Biomass Bioenergy 26, 485–495. https://doi.org/10.1016/J.BIOMBIOE.2003.08.008.

Mosbæk, F., Kjeldal, H., Mulat, D.G., Albertsen, M., Ward, A.J., Feilberg, A., Nielsen, J.L., 2016. Identification of syntrophic acetate-oxidizing bacteria in anaerobic digesters by combined protein-based stable isotope probing and metagenomics. ISME J. 10, 2405–2418. https://doi.org/10.1038/ismej.2016.39.

Mullet, M., Boursiquot, S., Abdelmoula, M., Génin, J.M., Ehrhardt, J.J., 2002. Surface chemistry and structural properties of mackinawite prepared by reaction of sulfide ions with metallic iron. Geochim. Cosmochim. Acta 66, 829–836. https://doi.org/10.1016/S0016-7037(01)00805-5.

Nakasaki, K., Koyama, M., Maekawa, T., Fujita, J., 2019. Changes in the microbial community during the acclimation process of anaerobic digestion for treatment of synthetic lipid-rich wastewater. J. Biotechnol. 306, 32–37. https://doi.org/10.1016/J.JBIOTEC.2019.09.003.

Ning, J., Zheng, Y., Young, D., Brown, B., Nesic, S., 2013. A thermodynamic study of hydrogen sulfide corrosion of mild steel. In: CORROSION 2013. OnePetro.

Niu, L., Song, L., Dong, X., 2008. Proteiniborus ethanoligenes gen. nov., sp. nov., an anaerobic protein-utilizing bacterium. Int. J. Syst. Evol. Microbiol. 58, 12–16. https://doi.org/10.1099/IJS.0.65108-0/CITE/REFWORKS.

Ohfuji, H., Rickard, D., 2006. High resolution transmission electron microscopic study of synthetic nanocrystalline mackinawite. Earth Planet. Sci. Lett. 241, 227–233. https://doi.org/10.1016/J.EPSL.2005.10.006.

Organization of the United Nations (FAO), 2020. The State of World Fisheries and Aquaculture 2020. In brief. In: The State of World Fisheries and Aquaculture 2020. In brief. FAO. https://doi.org/10.4060/CA9231EN.

Palomo-Briones, R., Xu, J., Spirito, C.M., Usack, J.G., Trondsen, L.H., Guzman, J.J.L., Angenent, L.T., 2022. Near-neutral pH increased n-caprylate production in a microbiome with product inhibition of methanogenesis. Chem. Eng. J. 446, 137170 https://doi.org/10.1016/J.CEJ.2022.137170.

Park, J.H., Kang, H.J., Park, K.H., Park, H.D., 2018. Direct interspecies electron transfer via conductive materials: a perspective for anaerobic digestion applications. Bioresour. Technol. 254, 300–311. https://doi.org/10.1016/J.BIORTECH.2018.01.095.

Perman, E., Schnürer, A., Björn, A., Moestedt, J., 2022. Serial anaerobic digestion improves protein degradation and biogas production from mixed food waste. Biomass Bioenergy 161, 106478. https://doi.org/10.1016/J.BIOMBIOE.2022.106478.

Pervin, H.M., Dennis, P.G., Lim, H.J., Tyson, G.W., Batstone, D.J., Bond, P.L., 2013. Drivers of microbial community composition in mesophilic and thermophilic temperature-phased anaerobic digestion pre-treatment reactors. Water Res. 47, 7098–7108. https://doi.org/10.1016/J.WATRES.2013.07.053.

Picard, A., Gartman, A., Clarke, D.R., Girguis, P.R., 2018. Sulfate-reducing bacteria influence the nucleation and growth of mackinawite and greigite. Geochim. Cosmochim. Acta 220, 367–384. https://doi.org/10.1016/J.GCA.2017.10.006.

Poszytek, K., Pyzik, A., Sobczak, A., Lipinski, L., Sklodowska, A., Drewniak, L., 2017. The effect of the source of microorganisms on adaptation of hydrolytic consortia dedicated to anaerobic digestion of maize silage. Anaerobe. https://doi.org/10.1016/j.anaerobe.2017.02.011.

Qi, Q., Sun, C., Zhang, J., He, Y., Wah Tong, Y., 2021. Internal enhancement mechanism of biochar with graphene structure in anaerobic digestion: the bioavailability of trace elements and potential direct interspecies electron transfer. Chem. Eng. J. 406, 126833 https://doi.org/10.1016/J.CEJ.2020.126833.

Roberts, A.P., Liu, Q., Rowan, C.J., Chang, L., Carvallo, C., Torrent, J., Horng, C., 2006. Characterization of hematite (α-Fe2O3), goethite (α-FeOOH), greigite (Fe3S4), and pyrrhotite (Fe7S8) using first-order reversal curve diagrams. J. Geophys. Res. Solid Earth 111.

Roldan, A., Santos-Carballal, D., De Leeuw, N.H., 2013. A comparative DFT study of the mechanical and electronic properties of greigite Fe3S4 and magnetite Fe3O4. J. Chem. Phys. 138, 204712 https://doi.org/10.1063/1.4807614.

Sarker, S., 2020. By-products of fish-oil refinery as potential substrates for biogas production in Norway: a preliminary study. Results Eng. https://doi.org/10.1016/j.rineng.2020.100137.

Shakeri Yekta, S., Liu, T., Axelsson Bjerg, M., Šafarič, L., Karlsson, A., Björn, A., Schnürer, A., 2019. Sulfide level in municipal sludge digesters affects microbial community response to long-chain fatty acid loads. Biotechnol. Biofuels 12, 1–15. https://doi.org/10.1186/S13068-019-1598-1/FIGURES/7.

Shiratori, H., Ohiwa, H., Ikeno, H., Ayame, S., Kataoka, N., Miya, A., Beppu, T., Ueda, K., 2008. Lutispora thermophila gen. nov., sp. nov., a thermophilic, spore-forming bacterium isolated from a thermophilic methanogenic bioreactor digesting municipal solid wastes. Int. J. Syst. Evol. Microbiol. 58, 964–969. https://doi.org/10.1099/IJS.0.65490-0/CITE/REFWORKS.

Sikora, A., Detman, A., Chojnacka, A., Błaszczyk, M.K., 2017. Anaerobic digestion: I. A common process ensuring energy flow and the circulation of matter in ecosystems. II. A tool for the production of gaseous biofuels. Ferment. Process. 14, 271.

Skyllberg, U., Persson, A., Tjerngren, I., Kronberg, R.M., Drott, A., Meili, M., Björn, E., 2021. Chemical speciation of mercury, sulfur and iron in a dystrophic boreal lake sediment, as controlled by the formation of mackinawite and framboidal pyrite. Geochim. Cosmochim. Acta 294, 106–125. https://doi.org/10.1016/J.GCA.2020.11.022.

Solli, L., Schnürer, A., Horn, S.J., 2018. Process performance and population dynamics of ammonium tolerant microorganisms during co-digestion of fish waste and manure. Renew. Energy 125, 529–536.

Stams, A.J.M., Plugge, C.M., 2009. Electron transfer in syntrophic communities of anaerobic bacteria and archaea. Nat. Rev. Microbiol. https://doi.org/10.1038/nrmicro2166.

Stevens, J.R., Newton, R.W., Tlusty, M., Little, D.C., 2018. The rise of aquaculture by-products: increasing food production, value, and sustainability through strategic utilisation. Mar. Policy 90, 115–124. https://doi.org/10.1016/J.MARPOL.2017.12.027.

Su, L., Zhen, G., Zhang, L., Zhao, Y., Niu, D., Chai, X., 2015. The use of the core–shell structure of zero-valent iron nanoparticles (NZVI) for long-term removal of sulphide in sludge during anaerobic digestion. Environ. Sci. Process. Impacts 17, 2013–2021. https://doi.org/10.1039/C5EM00470E.

Treu, L., Tsapekos, P., Peprah, M., Campanaro, S., Giacomini, A., Corich, V., Kougias, P. G., Angelidaki, I., 2019. Microbial profiling during anaerobic digestion of cheese whey in reactors operated at different conditions. Bioresour. Technol. 275, 375–385. https://doi.org/10.1016/J.BIORTECH.2018.12.084.

Trutschel, L.R., Chadwick, G.L., Kruger, B., Blank, J.G., Brazelton, W.J., Dart, E.R., Rowe, A.R., 2022. Investigation of microbial metabolisms in an extremely high pH marine-like terrestrial serpentinizing system: Ney Springs. Sci. Total Environ. 836, 155492 https://doi.org/10.1016/J.SCITOTENV.2022.155492.

van Dongen, B.E., Roberts, A.P., Schouten, S., Jiang, W.T., Florindo, F., Pancost, R.D., 2007. Formation of iron sulfide nodules during anaerobic oxidation of methane. Geochim. Cosmochim. Acta 71, 5155–5167. https://doi.org/10.1016/J.GCA.2007.08.019.

Vasiliev, I., Franke, C., Meeldijk, J.D., Dekkers, M.J., Langereis, C.G., Krijgsman, W., 2008. Putative greigite magnetofossils from the Pliocene epoch. Nat. Geosci. 1, 782–786. https://doi.org/10.1038/ngeo335.

Wagner, T., Koch, J., Ermler, U., Shima, S., 2017. Methanogenic heterodisulfide reductase (HdrABC-MvhAGD) uses two noncubane [4Fe-4S] clusters for reduction. Science 357, 699–703. https://doi.org/10.1126/SCIENCE.AAN0425/SUPPL_FILE/AAN0425_WAGNER_SM.PDF.

Wan, H., Wang, F., Chen, Y., Zhao, Z., Zhang, G., Dou, M., Xue, B., 2021. Enhanced Reactive Red 2 anaerobic degradation through improving electron transfer efficiency by nano-Fe3O4 modified granular activated carbon. Renew. Energy 179, 696–704. https://doi.org/10.1016/J.RENENE.2021.07.046.

Wang, Q., Chen, T., 2022. Oilfield iron sulfide scale formation and mitigation. Water-Formed Depos. 307–323. https://doi.org/10.1016/B978-0-12-822896-8.00028-5.

Wang, W., Lee, D.J., 2021. Direct interspecies electron transfer mechanism in enhanced methanogenesis: a mini-review. Bioresour. Technol. 330, 124980 https://doi.org/10.1016/J.BIORTECH.2021.124980.

Wang, D., Han, Y., Han, H., Li, K., Xu, C., Zhuang, H., 2018. New insights into enhanced anaerobic degradation of Fischer-Tropsch wastewater with the assistance of magnetite. Bioresour. Technol. 257, 147–156.

Wang, G., Li, Q., Gao, X., Wang, X.C., 2018. Synergetic promotion of syntrophic methane production from anaerobic digestion of complex organic wastes by biochar: performance and associated mechanisms. Bioresour. Technol. 250, 812–820. https://doi.org/10.1016/J.BIORTECH.2017.12.004.

Wang, H., Zhu, X., Yan, Q., Zhang, Y., Angelidaki, I., 2020. Microbial community response to ammonia levels in hydrogen assisted biogas production and upgrading process. Bioresour. Technol. 296, 122276 https://doi.org/10.1016/j.biortech.2019.122276.

Wang, S., Han, Y., Lu, X., Zhi, Z., Zhang, R., Cai, T., Zhang, Z., Qin, X., Song, Y., Zhen, G., 2021. Microbial mechanism underlying high methane production of coupled alkali-microwave–H2O2–oxidation pretreated sewage sludge by in-situ bioelectrochemical regulation. J. Clean. Prod. 305, 127195 https://doi.org/10.1016/J.JCLEPRO.2021.127195.

Wang, Z., Wang, T., Si, B., Watson, J., Zhang, Y., 2021. Accelerating anaerobic digestion for methane production: potential role of direct interspecies electron transfer. Renew. Sust. Energ. Rev. 145, 111069 https://doi.org/10.1016/j.rser.2021.111069.

Wu, J., Niu, Q., Li, L., Hu, Y., Mribet, C., Hojo, T., Li, Y.Y., 2018. A gradual change between methanogenesis and sulfidogenesis during a long-term UASB treatment of sulfate-rich chemical wastewater. Sci. Total Environ. 636, 168–176. https://doi.org/10.1016/J.SCITOTENV.2018.04.172.

Xia, Y., Wang, Yubo, Wang, Yi, Chin, F.Y.L., Zhang, T., 2016. Cellular adhesiveness and cellulolytic capacity in Anaerolineae revealed by omics-based genome interpretation. Biotechnol. Biofuels 9, 1–13.

Xing, L., Zhang, W., Gu, M., Yin, Q., Wu, G., 2020. Microbial interactions regulated by the dosage of ferroferric oxide in the co-metabolism of organic carbon and sulfate. Bioresour. Technol. 296, 122317 https://doi.org/10.1016/J.BIORTECH.2019.122317.

Yamada, T., Sekiguchi, Y., Hanada, S., Imachi, H., Ohashi, A., Harada, H., Kamagata, Y., 2006. Anaerolinea thermolimosa sp. nov., Levilinea saccharolytica gen. nov., sp. nov. and Leptolinea tardivitalis gen. nov., sp. nov., novel filamentous anaerobes, and description of the new classes Anaerolineae classis nov. and Caldilineae classis nov. in the. Int. J. Syst. Evol. Microbiol. 56, 1331–1340.

Yan, Z., Ferry, J.G., 2018. Electron bifurcation and confurcation in methanogenesis and reverse methanogenesis. Front. Microbiol. 9, 1322. https://doi.org/10.3389/FMICB.2018.01322/BIBTEX.

Yenigün, O., Demirel, B., 2013. Ammonia inhibition in anaerobic digestion: a review. Process Biochem. 48, 901–911. https://doi.org/10.1016/J.PROCBIO.2013.04.012.

Yutin, N., Galperin, M.Y., 2013. A genomic update on clostridial phylogeny: Gram-negative spore formers and other misplaced clostridia. Environ. Microbiol. 15, 2631–2641. https://doi.org/10.1111/1462-2920.12173/SUPPINFO.

Zhang, J., Zeng, D., Xu, C., Gao, M., 2015. Effect of low-frequency magnetic field on formation of pigments of Monascus purpureus. Eur. Food Res. Technol. https://doi.org/10.1007/s00217-014-2358-x.

Zhang, L., Loh, K.C., Zhang, J., 2019. Jointly reducing antibiotic resistance genes and improving methane yield in anaerobic digestion of chicken manure by feedstock microwave pretreatment and activated carbon supplementation. Chem. Eng. J. 372, 815–824. https://doi.org/10.1016/J.CEJ.2019.04.207.

Zhang, W., Li, L., Wang, X., Xing, W., Li, R., Yang, T., Lv, D., 2020. Role of trace elements in anaerobic digestion of food waste: process stability, recovery from volatile fatty acid inhibition and microbial community dynamics. Bioresour. Technol. 315, 123796 https://doi.org/10.1016/J.BIORTECH.2020.123796.

Zhang, L., Ban, Q., Li, J., Zhang, S., 2022. An enhanced excess sludge fermentation process by anthraquinone-2-sulfonate as electron shuttles for the biorefinery of zero-carbon hydrogen. Environ. Res. 210, 113005 https://doi.org/10.1016/J.ENVRES.2022.113005.

Zhao, Z., Zhang, Y., Holmes, D.E., Dang, Y., Woodard, T.L., Nevin, K.P., Lovley, D.R., 2016. Potential enhancement of direct interspecies electron transfer for syntrophic metabolism of propionate and butyrate with biochar in up-flow anaerobic sludge blanket reactors. Bioresour. Technol. 209, 148–156. https://doi.org/10.1016/J.BIORTECH.2016.03.005.

Zhao, Z., Wang, J., Li, Y., Zhu, T., Yu, Q., Wang, T., Liang, S., Zhang, Y., 2020. Why do DIETers like drinking: metagenomic analysis for methane and energy metabolism during anaerobic digestion with ethanol. Water Res. 171 https://doi.org/10.1016/J.WATRES.2019.115425.

Zhao, Z., Li, Y., Zhang, Y., 2021. Engineering enhanced anaerobic digestion: benefits of ethanol fermentation pretreatment for boosting direct interspecies electron transfer. Energy 228, 120643. https://doi.org/10.1016/J.ENERGY.2021.120643.

Zieliński, M., Zielińska, M., Cydzik-Kwiatkowska, A., Rusanowska, P., Dębowski, M., 2021. Effect of static magnetic field on microbial community during anaerobic digestion. Bioresour. Technol. https://doi.org/10.1016/j.biortech.2020.124600.